NASA TECHNICAL NOTE

NASA TN D-6042

C. 1

NASA TN D-6042



# THERMAL FEASIBILITY OF USING METHANE OR HYDROGEN FUEL FOR DIRECT COOLING OF A FIRST-STAGE TURBINE STATOR

*by Raymond S. Colladay*

*Lewis Research Center*

*Cleveland, Ohio 44135*

NATIONAL AERONAUTICS AND SPACE ADMINISTRATION • WASHINGTON, D. C. • OCTOBER 1970

| | | |
|---|---|---|
| 1. Report No. NASA TN D-6042 | 2. Government Accession No. | 3. Recipient's Catalog No. |
| 4. Title and Subtitle THERMAL FEASIBILITY OF USING METHANE OR HYDROGEN FUEL FOR DIRECT COOLING OF A FIRST-STAGE TURBINE STATOR | | 5. Report Date October 1970 |
| | | 6. Performing Organization Code |
| 7. Author(s) Raymond S. Colladay | | 8. Performing Organization Report No. E-5701 |
| 9. Performing Organization Name and Address Lewis Research Center National Aeronautics and Space Administration Cleveland, Ohio 44135 | | 10. Work Unit No. 720-03 |
| | | 11. Contract or Grant No. |
| 12. Sponsoring Agency Name and Address National Aeronautics and Space Administration Washington, D.C. 20546 | | 13. Type of Report and Period Covered Technical Note |
| | | 14. Sponsoring Agency Code |
| 15. Supplementary Notes | | |

16. Abstract

The feasibility of cooling the first-stage turbine stator directly with cryogenic fuels is investigated based on a numerical heat transfer analysis of methane- and hydrogen-cooled vanes. An insulation barrier between the fuel cooling passages and the external vane surface was required to prevent adverse cooling conditions. The cooling configuration analyzed was that of tubular cooling passages embedded in insulation material surrounded by an outer vane shell. The results indicated that the turbine stator vanes could be adequately cooled with methane or hydrogen fuel at a $2490^{\circ}$ F (1639 K) local-hot-spot gas temperature.

| | | | |
|---|---|---|---|
| 17. Key Words (Suggested by Author(s)) Fuel cooling Turbine vanes Methane Hydrogen | | 18. Distribution Statement Unclassified - unlimited | |
| 19. Security Classif. (of this report) Unclassified | 20. Security Classif. (of this page) Unclassified | 21. No. of Pages 25 | 22. Price* $3.00 |

*For sale by the Clearinghouse for Federal Scientific and Technical Information
Springfield, Virginia 22151

# THERMAL FEASIBILITY OF USING METHANE OR HYDROGEN FUEL FOR DIRECT COOLING OF A FIRST-STAGE TURBINE STATOR

by Raymond S. Colladay

Lewis Research Center

## SUMMARY

To evaluate the effectiveness of cooling the first-stage turbine stator of a typical supersonic aircraft engine directly with liquid-methane or liquid-hydrogen fuel, the steady-state, two-dimensional temperature distribution at the midspan of the stator vane was determined numerically for cruise and takeoff conditions. The analysis was applied to a turbine for an aircraft cruising at Mach 3 at an altitude of 75 000 feet (22.8 km) with a turbine inlet temperature of $2270^{\circ}$ F (1517 K). The external gas temperature was based on a circumferential-hot-spot temperature of $2490^{\circ}$ F (1639 K).

The cooling configuration which met the assumed maximum metal temperatures and metal temperature variation consistent with vane life requirements is presented for relatively simple tubular spanwise coolant passages. An insulation barrier between the coolant passages and the outer vane surface was necessary to control the vane temperatures and protect the fuel tubes from overheating. Excessive fuel surface temperatures could cause fuel cracking and/or carburization in the case of methane cooling.

Vane surface temperatures on both the gas side and coolant side were greatest for the case of methane cooling. These maximum surface temperatures were respectively, $1802^{\circ}$, $1938^{\circ}$, $1070^{\circ}$, and $441^{\circ}$ F (1257, 1332, 850, and 500 K) for gas-side cruise and takeoff, and coolant-side cruise and takeoff. The resulting rise in the temperature of the methane fuel passing through the first stage stator was $340^{\circ}$ F (189 K) for cruise conditions. Hydrogen proved to be slightly more effective than methane for this cooling application.

Difficulties arise in cooling a thin trailing edge directly with fuel because of the lack of sufficient thickness to accommodate the coolant passage and insulation. Consideration was given to several alternatives for cooling the trailing-edge region; namely, increasing the trailing-edge thickness and wedge angle, and introducing a heat pipe in this region.

# INTRODUCTION

The feasibility of direct cooling of first-stage turbine stator vanes with cryogenic fuels was investigated based on a numerical heat transfer analysis of methane- and hydrogen-cooled vanes.

Turbine inlet temperatures have increased considerably in recent years to meet the requirements of advanced high-performance turbojet engines. As a result, some means of cooling the turbine vanes and blades is required in order to maintain reasonable material temperatures and life expectancy of the turbine components. The usual cooling method is to bleed air from the compressor exit and route it through the internal passages of the turbine blades and vanes. However, with increased compressor exit temperatures associated with the high-pressure-ratio engines currently proposed, severe limitations on the potential of using compressor bleed air to directly cool turbine blades and vanes are imposed.

Studies, such as reference 1, have considered utilizing some of the heat sink available in the fuel to cool the compressor bleed air. However, if the turbine vanes and blades could be cooled directly with the fuel, the added weight of a fuel-to-air heat exchanger could be eliminated. A direct fuel cooling method has other advantages which contribute to the overall engine cycle efficiency; namely, (1) less compressor bleed air is required, (2) the gas-stream temperature drop across a fuel-cooled stator (or rotor) is reduced since no mixing of the coolant with the external gas takes place, and (3) the heat energy transferred to the fuel is recovered through the higher enthalpy of the fuel entering the combustor. Possible disadvantages of such a cooling scheme are fuel fouling and the potential hazards associated with routing the fuel through the high-temperature vanes.

Previous investigations (refs. 1 and 2) have shown that liquid-methane fuel could improve the performance of commercial supersonic transports, especially when engines are used which impose high turbine cooling loads. Although hydrogen would not be expected to be used in an SST, there is some current interest in hydrogen fueled gas turbine engines. The feasibility of hydrogen cooling was investigated for the same vane and engine conditions as for methane cooling. This approach provided a comparison of the relative cooling capabilities for the two fuels.

This report is a study of the feasibility of using methane and hydrogen fuel directly to cool the first-stage stator of an SST aircraft turbine. The success of such a cooling scheme depends on the ability to maintain surface temperatures in contact with the fuel below a value known to cause carburization and fuel cracking (in the case of methane), while avoiding large temperature gradients in the stator vane shell material caused by the large differences between the fuel temperature and the desired vane metal temperature. Due to these design restrictions, the analysis was based upon the assumption that a thermal barrier would be required between the fuel and the external vane surface.

The conditions for the analysis were based on an engine designed for a Mach 3 flight at a cruise altitude of 75 000 feet (22.8 km) with an average turbine inlet temperature (to the first-stage vanes) of $2270^{\circ}$ F (1517 K). The gas temperature design point was based on a circumferential hot-spot temperature of $2490^{\circ}$ F (1639 K). The engine compressor pressure ratio was 3.67 for cruise conditions. Other limiting conditions imposed were an $1850^{\circ}$ F (1283 K) maximum vane surface temperature for cruise conditions and a $1200^{\circ}$ F (922 K) maximum coolant passage surface temperature. It was assumed that the methane enters the first-stage stator at $0^{\circ}$ F (255 K) for cruise and $-116^{\circ}$ F (191 K) for takeoff at a pressure of 700 psia (4.83 $MN/m^2$), and for hydrogen the same respective values were $-215^{\circ}$ F (136 K), $-275^{\circ}$ F (103 K), and 300 psia (2.07 $MN/m^2$). All the fuel required by the combustor was routed through the first-stage turbine stator.

This investigation was based on the engine conditions just given (from ref. 3). No attempt was made to establish the upper limit of the permissible turbine inlet gas temperature with this method of cooling.

## CONDITIONS AND METHOD OF ANALYSIS

In the following sections, the design conditions and a description of the heat transfer analysis used in evaluating the proposed fuel cooling scheme are presented.

Turbine and engine conditions. - The basic design point for the heat transfer analysis of the first-stage turbine stator vane was obtained from reference 3. Table I summarizes

TABLE I. - ENGINE OPERATING CONDITIONS

| Condition | Cruise | Takeoff |
|---|---|---|
| Flight Mach number | 3 | ------------ |
| Flight altitude, ft (km) | 75 000 (22.8) | ------------ |
| JP fuel-air ratio | 0.0169 | 0.0261 |
| Compressor inlet airflow, lbm/sec (kg/sec) | 182.6 (82.7) | 475 (215.5) |
| Average turbine inlet gas temperature, $^{\circ}$F (K) | 2270 (1517) | 2270 (1517) |
| Turbine inlet gas flow, lbm/sec (kg/sec) | 148.0 (67.1) | 370.3 (169.0) |
| Pattern factor,[a] $(T_{t,max} - \overline{T}_t)/(\overline{T} - \overline{T}_{c,e})$ | 0.2 | 0.2 |
| Turbine inlet total pressure, psia ($MN/m^2$) | 51.1 (0.352) | 131.3 (0.905) |
| Compressor total pressure ratio | 3.67 | 9.49 |

[a]Symbols are defined in appendix A.

TABLE II. - FIRST-STAGE STATOR VANES

| | |
|---|---|
| Number of vanes | 64 |
| Trailing-edge thickness, in. (cm) | 0.075 (0.191) |
| Leading-edge radius, in. (cm) | 0.2 (0.508) |
| Vane height, in. (cm) | 5.3 (13.46) |
| Chord length, in. (cm) | 3.75 (9.53) |

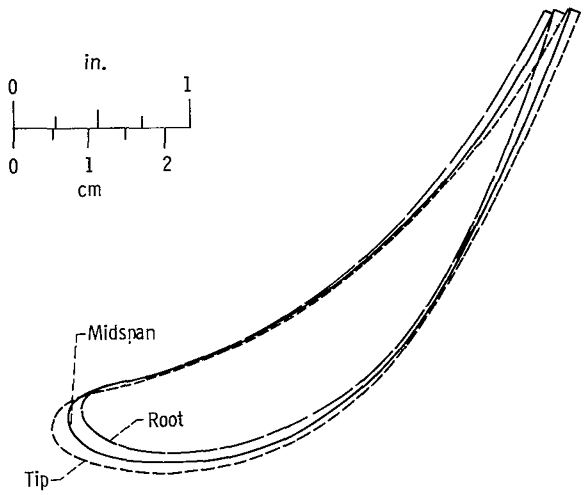


Figure 1. - First-stage stator vane. (From ref. 3.)

marizes the pertinent engine operating conditions for cruise and takeoff needed for this study, while table II lists some of the dimensions of the first-stage stator vane analyzed. Figure 1 shows the stator vane profile for this engine. Fuel flow rates for methane and hydrogen were adjusted to meet the same combustor requirements (and therefore the same engine operating conditions) as those based on JP fuel-air ratios by ratioing the JP values given in table I with the various fuel heating values. Heat of combustion values for methane (99 percent pure), hydrogen, and JP fuel were obtained from reference 4, and enthalpy data for methane was obtained from reference 5. The temperature of the methane entering the combustor was assumed to be $1000^{\circ}$ F (811 K). Table III summarizes the fuel flow rates used in this study. All the fuel required by the combustor was passed through the first-stage stator by dividing it equally among the 64 vanes.

Some heating of the fuel takes place as it passes from the storage tanks (maintained at a temperature of $-259^{\circ}$ F (112 K)) to the first-stage turbine stator. Methane entering the root section of the stator vanes was assumed to be at a temperature of $0^{\circ}$ F (255 K) for cruise and $-116^{\circ}$ F (191 K) (critical temperature) for takeoff. Based on the same heat loads upstream of the stator, the hydrogen fuel enters the vane root section at tem-

TABLE III. - FUEL FLOW RATE

| Flight condition | JP fuel | Methane | Hydrogen |
|---|---|---|---|
| | Flow rate, w, lbm/sec (kg/sec) | | |
| Cruise | 3.09 (1.40) | 2.64 (1.20) | 1.12 (0.51) |
| Takeoff | 12.40 (5.62) | 10.60 (4.81) | 4.50 (2.04) |

peratures of -215° F (136 K) and -275° F (103 K) for cruise and takeoff, respectively, assuming a fuel tank storage temperature of -423° F (20 K).

The fuel in the cooling lines was assumed to be pumped to pressures of 700 psia (4.83 $MN/m^2$) and 300 psia (2.07 $MN/m^2$) for methane and hydrogen, respectively. These pressures were chosen to be in the slightly supercritical range.

In view of the fact that combustor radial and circumferential gas-temperature profiles influence vane metal temperatures and life, the design point for the external gas temperature was assumed to be the local-hot-spot temperature typical for the given combustor. For the engine operating conditions given in table I, the design hot-spot temperature was 2490° F (1639 K), approximately constant over the chord length. This corresponds to a combustor pattern factor (ratio of the difference between the hot-spot and average burner outlet temperatures to the difference between the average burner outlet and compressor exit temperatures) of 0.20.

Heat transfer analysis. - The local gas-to-vane heat-transfer coefficient distribution $h_g$ around the vane, hereinafter called the local outside heat transfer coefficient, is given in reference 3 for cruise conditions. The local values of $h_g$ for takeoff were computed by approximating the suction and pressure surfaces as flat plates where the heat transfer coefficient for turbulent flow is proportional to $Re^{0.8}$. Because the total gas temperature is the same for both cruise and takeoff conditions and if approximately the same vane surface temperatures are assumed for both flight conditions, the ratio of the heat transfer coefficients for cruise and takeoff is equal to the ratio of the respective gas flow rates (from table I) to the 0.8 power.

The same percent increase in $h_g$ from cruise to takeoff was assumed over the entire vane. As a result, the leading-edge $h_g$ for takeoff is somewhat higher than would be calculated by assuming laminar free-stream conditions where the leading-edge correlation involves $Re^{0.5}$. The distribution of $h_g$ for takeoff conditions is given in figure 2.

The average vane-to-coolant heat transfer coefficient $\bar{h}_c$, subsequently referred to as the inside heat transfer coefficient, was obtained by using the following correlation for turbulent flow in tubes (ref. 6).

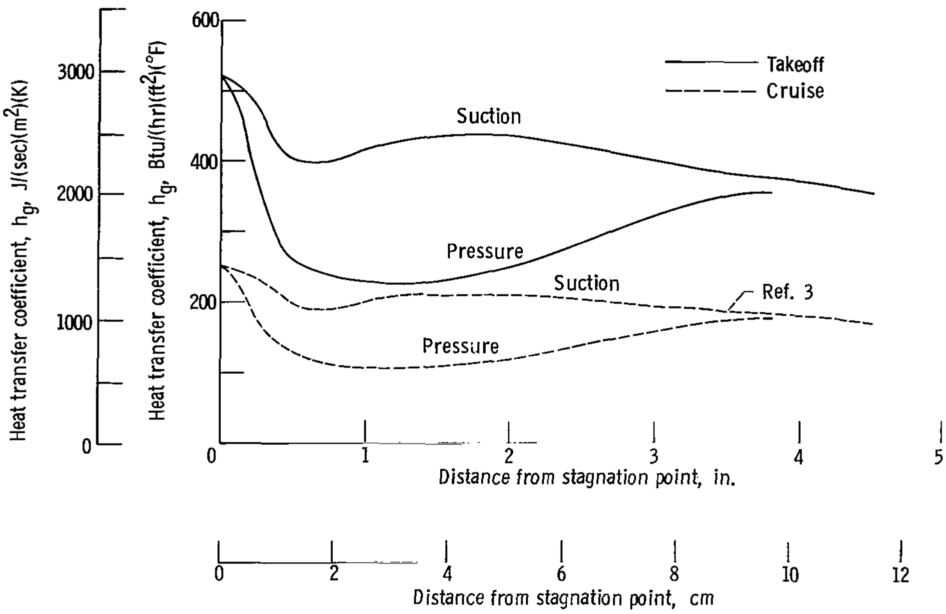


Figure 2. - Gas-to-blade heat transfer coefficient.

$$h_c = \frac{k_b}{D} 0.027 (Re_b)^{0.8} (Pr_b)^{1/3} \left(\frac{\mu_b}{\mu_s}\right)^{0.14} \tag{1}$$

Transport properties for methane were obtained from reference 7 and for hydrogen from references 8 to 10. The viscosity ratio in this correlation corrects for the large differences between the surface temperature of the cooling passages and the bulk temperature of the fuel.

A numerical solution of the steady-state, two-dimensional heat conduction equation was used to generate the temperature distribution at the midspan of the vane. A brief description of the numerical method (ref. 11) is given in appendix B. The node breakup for this analysis is shown in figure 3.

Average thermal conductivity values were used for the vane and insulation materials, and no variation with temperature was considered. A thermal conductivity of 12 Btu per hour per foot per $^{\circ}$F (20.8 J/(m)(sec)(K)) for the vane shell was assumed as a typical value for various high-temperature alloy materials at a temperature of 1800$^{\circ}$ F (1255 K). The heat flux in the spanwise direction was assumed to be negligible compared to that in the plane normal to the spanwise direction. The contact resistance of the interface between different materials was also neglected.

The following boundary conditions were required in the numerical solution: (1) local outside heat transfer coefficient $h_g$, (2) external gas temperature, (3) inside heat trans-

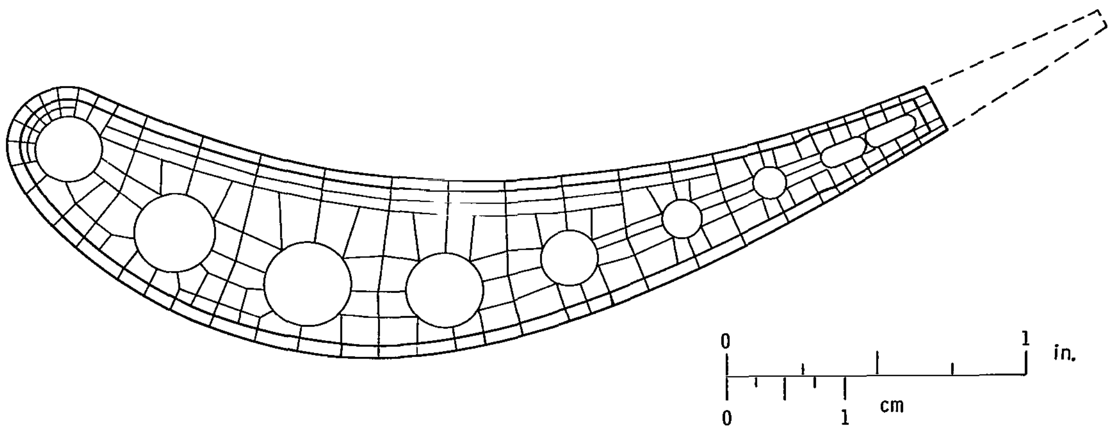


Figure 3. - Node breakup of stator vane.

fer coefficient for each coolant passage $\bar{h}_c$, and (4) midspan bulk temperature of the coolant in each passage. Since the last two boundary conditions depend on the resulting temperature distribution and overall heat balance, they are a priori unknown. Thus, it was necessary to resort to the following iterative procedure: (1) a midspan bulk temperature was assumed for each cooling passage; (2) inside heat transfer coefficients were then calculated using equation (1) (after average tube surface temperatures were estimated in forming the viscosity ratio); (3) following the numerical solution of the heat conduction equation, the heat added to the fuel flowing through each passage was calculated from the following equation:

$$q_i = \sum_n \bar{h}_{c,i} A_{i,n} (T_n - T_{b,i})$$

where the summation over n is over all nodes which have areas $A_{i,n}$ adjacent to the coolant in the $i^{th}$ passage; (4) a new bulk temperature was then determined from

$$q_i = w_{c,i}(h_{ms} - h_o)_i$$

The procedure was then repeated until the change in the bulk temperature and estimated coolant passage surface temperature became arbitrarily small.

Methane-cooled vane. - To avoid fuel cracking and embrittlement caused by carburization, the surface temperature in contact with the methane should not be greater than about $1200^{\circ}$ F (922 K) at any spanwise location. Reference 12 indicates that considerable embrittlement of several high-temperature alloys tested occurred when the heated surface in contact with methane reached a temperature somewhere between $1200^{\circ}$ and $1800^{\circ}$ F (922 and 1255 K). Perhaps this $1200^{\circ}$ F (922 K) constraint can be relaxed when further information is gained regarding the temperature at which carbon diffusion into the metal becomes excessive. Also, for the long life requirements of commercial aircraft turbines operating at high inlet temperatures, the temperature gradients in the vane material must be small to avoid large thermal stresses.

As a result of these two thermal design requirements, the analysis was conducted based on the assumption that an insulation barrier would be required between the fuel (whose bulk temperature at midspan may be as low as $-110^{\circ}$ F (194 K)) and the vane shell. The coolant-side and gas-side surface temperatures are then controlled by the insulation barrier with the large temperature differences occurring across the insulation rather than across the vane shell structure. The particular cooling configuration analyzed was that of tubular cooling passages embedded in an insulation material surrounded by the outer vane shell.

Hydrogen-cooled vane. - Though carburization is not a factor when cooling the vane with hydrogen, there may be a problem with decarburization with hydrogen in contact with elevated surface temperatures. The conditions under which decarburization would occur are not well known. As a result, no limiting cooling passage temperature was assigned for the calculations with hydrogen cooling.

Shell material temperature limits. - The temperature criteria used to provide satisfactory vane design for an assumed 1000-hour-life requirement are described in reference 13.

The conductivity of the insulation material; the location, diameter, and number of cooling passages; and the number of fuel passes through the vane were all varied in the analysis in order to arrive at a cooling configuration which would meet the assumed temperature criteria of (1) maximum temperature difference within the outer vane shell of approximately $200^{\circ}$ F (111 K) for both cruise and takeoff conditions, (2) methane fuel-surface interface temperature less than approximately $1200^{\circ}$ F (922 K) at any spanwise location; (3) minimum temperature differences between takeoff and cruise conditions; (4) maximum surface temperature for cruise on the order of $1850^{\circ}$ F (1283 K). Surface temperatures approaching $2000^{\circ}$ F (1367 K) can be tolerated for short periods of time such as during takeoff and still maintain overall life requirements.

## RESULTS AND DISCUSSION

The heat transfer analysis described has been applied to a Mach 3 aircraft stator cooled directly with methane or hydrogen fuel. The feasibility of such a cooling scheme is discussed in the following sections.

Methane-cooled vane. - For the given vane and cooling configuration analyzed, the particular design which adequately met the temperature criteria discussed in the section

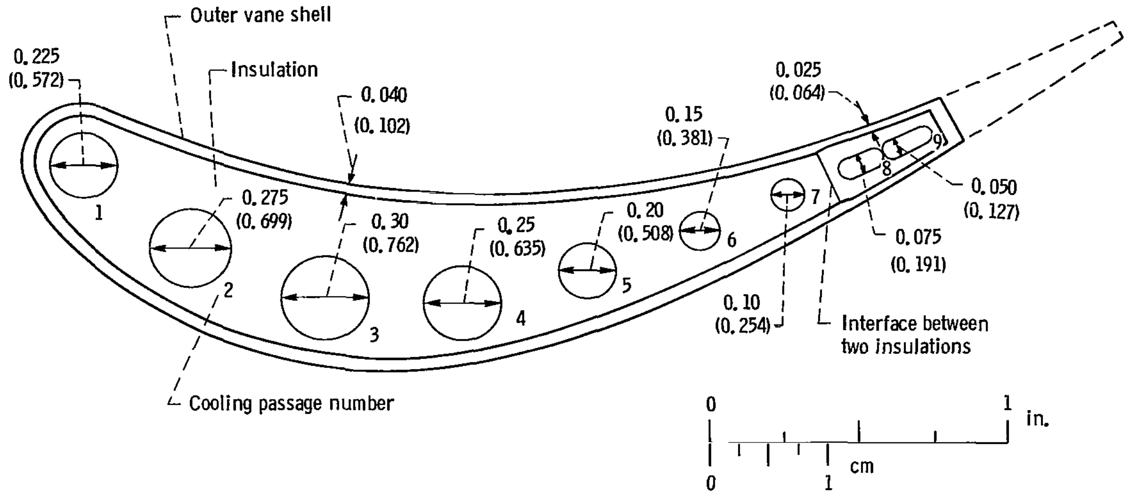


Figure 4. - Stator vane cooling configuration. (Dimensions are in inches (cm).)

Shell material temperature limits is shown in figure 4. Nine cooling passages (sealed with a thin tube to contain the coolant) are embedded in the insulation. Based on the thermal conductivity range required of the insulation, a felt or fibrous metal appears to be a satisfactory insulation material.

Notice that the cooling passages are shifted towards the suction surface. This reduces the large temperature differences that would otherwise exist between the suction and pressure surfaces.

The details of fabrication were not considered in this report except where they might affect heat transfer results. One method of fabrication might be to insert the core segment consisting of the cooling passages embedded in the insulation material into the vane shell and braze the contacting surfaces. In a later section, the effect on the vane temperature profile of a loss of braze contact is investigated.

In order to extend the cooling passages and accompanying insulation as far back into the trailing edge as possible without both overcooling this region and causing excessive inside surface temperatures, it was necessary to resort to insulation having a lower conductivity near the trailing edge than that used for the rest of the vane. However, even with this effort it was impossible to adequately cool the entire trailing-edge region of the given vane with fuel when minimum dimensions on the vane shell thickness and tube diameter of 0.025 and 0.050 inches (0.0635 and 0.127 cm), respectively, were imposed.

For the given vane design, the thermal conductivity values for the insulation in the two regions were 1.4 and 0.52 Btu/(hr)(ft)($^{o}$F) (2.42 and 0.90 J/(m)(sec)(K)), the latter values being for the trailing-edge region. The effects of this reduced thermal conductivity in the trailing-edge region are discussed later.

In order to satisfy the 1200$^{o}$ F (922 K) limit for the coolant-side surface tempera-

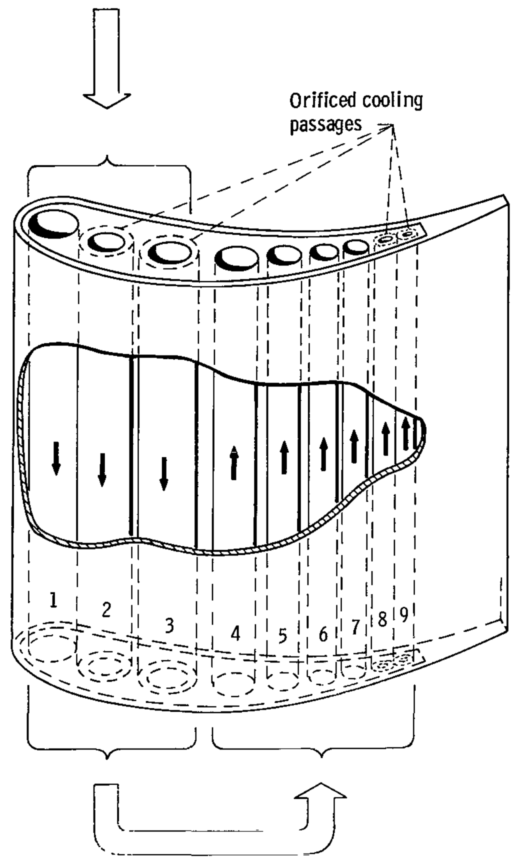


Figure 5. - Methane coolant path through vane.

ture, higher flow rates and, hence, larger inside heat transfer coefficients were required than could be achieved by routing the fuel through all nine passages in a single pass. Satisfactory temperatures were obtained by requiring all the fuel available for cooling a vane to pass from a common plenum through holes 1 to 3 on the first pass, then through holes 4 to 9 on a second pass. The flow path is shown in figure 5.

Also, in order to maintain as nearly as possible a constant outer surface temperature in the chordwise direction, it was necessary to orifice passages 2, 3, 8, and 9.

The resulting temperature distributions in the vane under cruise and takeoff conditions are shown in figures 6 and 7, respectively. Some representative temperatures in the insulation are given in figure 6.

At the leading edge, where the wall temperature gradient is maximum, the temperature difference across the vane shell was $48^{\circ}$ and $70^{\circ}$ F (27 and 39 K) for cruise and takeoff, respectively.

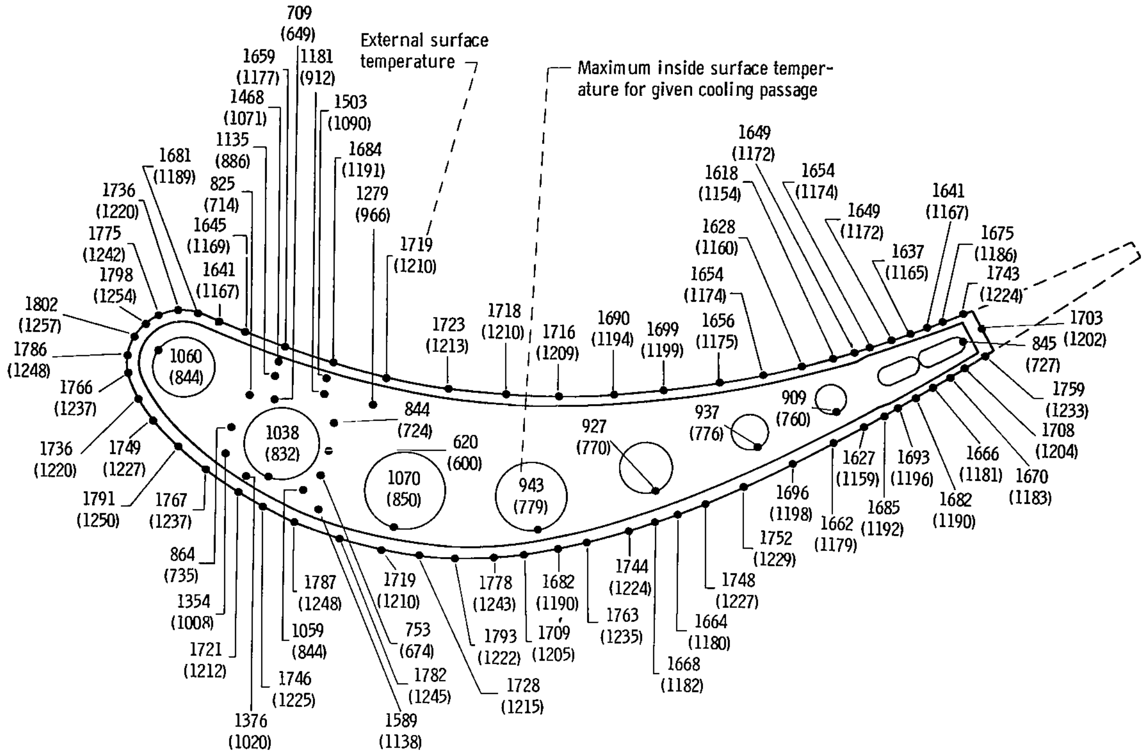


Figure 6. - Temperature distribution in methane-cooled vane under cruise conditions. (Temperatures are in °F (K).)

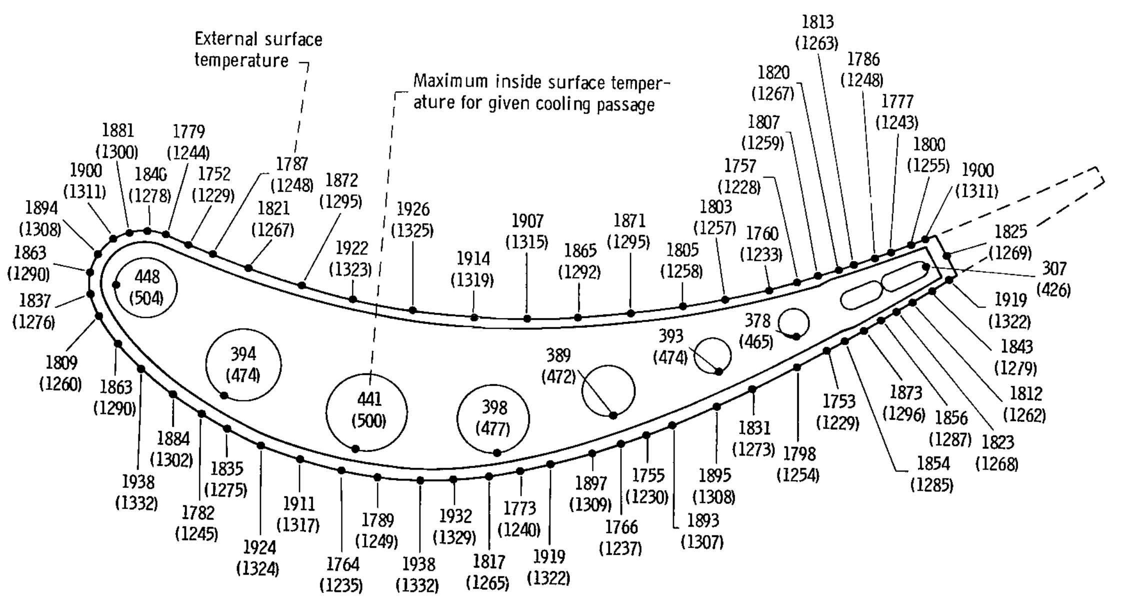


Figure 7. - Temperature distribution in methane-cooled vane under takeoff conditions. (Temperatures are in °F (K).)

The most difficult cooling requirement to meet was that of keeping the inside surface temperatures for cruise and the outside surface temperatures for takeoff both within their respective limits.

The temperature distribution shown is the result of eliminating the last 0.64 inch (1.63 cm) of the trailing edge and assuming a heat transfer coefficient on the truncated surface of 100 and 208 Btu/(hr)(ft$^2$)($^\circ$F) ($2.04\times10^6$ and $4.25\times10^6$ J/(hr)(m$^2$)(K)) for cruise and takeoff, respectively. Using the same cooling configuration without eliminating any of the trailing-edge section resulted in a temperature approaching 95 percent of the gas-stream temperature at a distance of 0.25 inch (0.635 cm) from the ninth cooling passage, for takeoff conditions.

With an insulation conductivity of 1.4 Btu/(hr)(ft)($^\circ$F) (2.42 J/(m)(sec)(K)) throughout the entire vane, the external surface temperatures opposite the eighth and ninth cooling passages were on the order of 250$^\circ$ F (139 K) lower at cruise than the corresponding temperatures given in figure 6. Further discussion of the trailing-edge problem appears in a later section.

The coolant flow, heat transfer coefficients, and midspan bulk temperatures for each of the nine cooling passages under both cruise and takeoff conditions are given in table IV. The relative coolant flow rate is the ratio of the fuel flowing through a given passage to the total flow through the vane, the latter being 1/64th of the total engine fuel flow rate.

The total heat added to the methane in cooling the 64 stator vanes to the temperature distribution for cruise and takeoff given in figures 6 and 7 resulted in a temperature rise in the methane of 340$^\circ$ and 135$^\circ$ F (189 and 75 K), respectively. The resulting drop in the external gas temperature across the first-stage stator was 13$^\circ$ and 9$^\circ$ F (7 and 5 K) for cruise and takeoff, respectively. In comparison, for cruise conditions, reference 3 reports a 70$^\circ$ F (39 K) gas temperature drop if compressor bleed air is used to cool the vane and then mixes with the external gas.

TABLE IV. - MIDSPAN CONDITIONS FOR METHANE FUEL

| Coolant passage | Relative coolant flow rate | Cruise | | Takeoff | | Cruise | | Takeoff | |
|---|---|---|---|---|---|---|---|---|---|
| | | Heat transfer coefficient | | | | Bulk temperature | | | |
| | | Btu/(hr)(ft$^2$)($^\circ$F) | J/(hr)(m$^2$)(K) | Btu/(hr)(ft$^2$)($^\circ$F) | J/(hr)(m$^2$)(K) | $^\circ$F | K | $^\circ$F | K |
| 1 | 0.30 | 295 | $6.03\times10^6$ | 1000 | $20.43\times10^6$ | 100 | 311 | -110 | 194 |
| 2 | .32 | 205 | 4.19 | 820 | 16.75 | 30 | 272 | -110 | 194 |
| 3 | .38 | 200 | 4.09 | 800 | 16.34 | 30 | 272 | -110 | 194 |
| 4 | .39 | 347 | 7.09 | 950 | 19.41 | 250 | 394 | -80 | 211 |
| 5 | .25 | 363 | 7.42 | 986 | 20.14 | 250 | 394 | -80 | 211 |
| 6 | .14 | 384 | 7.84 | 1050 | 21.45 | 260 | 400 | -70 | 217 |
| 7 | .07 | 445 | 9.09 | 1210 | 24.72 | 330 | 439 | -30 | 239 |
| 8 | .08 | 360 | 7.35 | 990 | 20.22 | 270 | 405 | -70 | 217 |
| 9 | .07 | 360 | 7.35 | 990 | 20.22 | 270 | 405 | -70 | 217 |

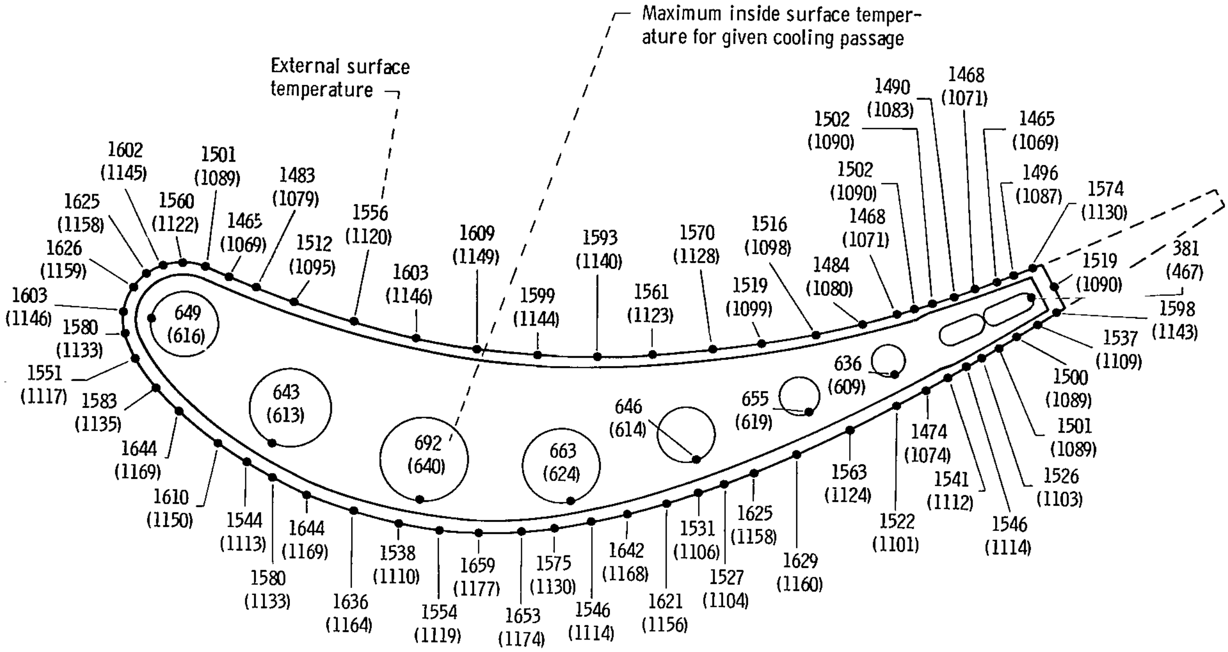


Figure 8. - Temperature distribution in hydrogen-cooled vane under cruise conditions. (Temperatures are in °F (K).)

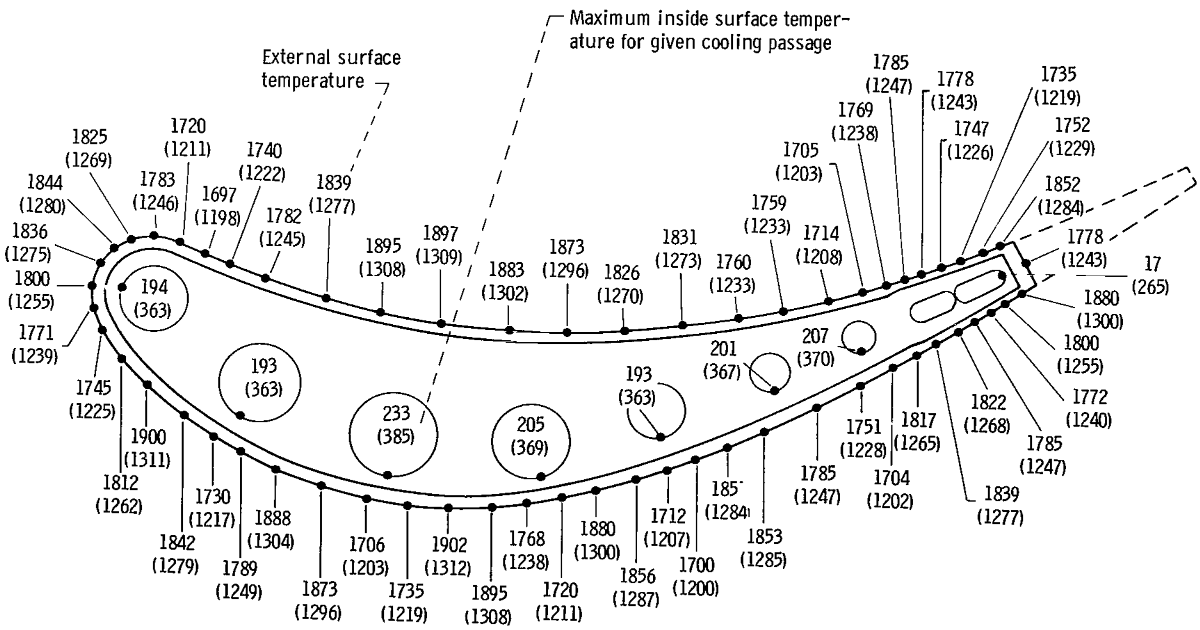


Figure 9. - Temperature distribution in hydrogen-cooled vane under takeoff conditions. (Temperatures are in °F (K).)

Hydrogen-cooled vane. - In cooling the vane with hydrogen fuel, the same cooling passage configuration was considered. However, satisfactory cooling was achieved by allowing all the fuel available for cooling the vane to flow through all nine passages in a single pass. In this case, passages 2 to 7 were orificed in order to reduce excessive leading-edge to midchord temperature differences by increasing the coolant flow rate through the leading-edge passage. For the given vane design, the thermal conductivity values for the insulation material were 0.48 and 1.37 Btu/(hr)(ft)($^{\circ}$F) (2.37 and 0.85 J/(m$^2$)(sec)(K)) for the trailing-edge region and for the remaining portion, respectively. The resulting temperature distributions for cruise and takeoff conditions are shown in figures 8 and 9, respectively. At the leading edge, the temperature difference across the vane shell was 60$^{\circ}$ and 74$^{\circ}$ F (33 and 41 K) for cruise and takeoff, respectively. The coolant flow, heat transfer coefficients, and midspan bulk temperatures for each of the nine cooling passages under both cruise and takeoff conditions are given in table V.

TABLE V. - MIDSPAN CONDITIONS FOR HYDROGEN FUEL

| Coolant passage | Relative coolant flow rate | Cruise | | Takeoff | | Cruise | | Takeoff | |
|---|---|---|---|---|---|---|---|---|---|
| | | Heat transfer coefficient | | | | Bulk temperature | | | |
| | | Btu/(hr)(ft$^2$)($^{\circ}$F) | J/(hr)(m$^2$)(K) | Btu/(hr)(ft$^2$)($^{\circ}$F) | J/(hr)(m$^2$)(K) | $^{\circ}$F | K | $^{\circ}$F | K |
| 1 | 0.175 | 481 | 9.83×10$^6$ | 1460 | 29.82×10$^6$ | -120 | 189 | -240 | 122 |
| 2 | .184 | 347 | 7.09 | 1060 | 21.65 | -140 | 178 | -250 | 117 |
| 3 | .218 | 341 | 6.97 | 1040 | 21.25 | -130 | 183 | -250 | 117 |
| 4 | .152 | 354 | 7.23 | 1080 | 22.06 | -120 | 189 | -240 | 122 |
| 5 | .097 | 370 | 7.56 | 1130 | 23.08 | -120 | 189 | -240 | 122 |
| 6 | .055 | 392 | 8.01 | 1190 | 24.31 | -110 | 194 | -230 | 128 |
| 7 | .025 | 460 | 9.40 | 1395 | 28.50 | -10 | 250 | -170 | 161 |
| 8 | .047 | 520 | 10.62 | 1580 | 32.28 | -130 | 183 | -250 | 117 |
| 9 | .047 | 520 | 10.62 | 1580 | 32.28 | -130 | 183 | -250 | 117 |

The temperature rise of the hydrogen in cooling the 64 stator vanes to the resulting temperature distribution, given in figures 8 and 9, was 165$^{\circ}$ and 63$^{\circ}$ F (92 and 35 K) for cruise and takeoff, respectively.

Trailing edge. - The inability to convectively cool the trailing-edge section of the given vane with fuel dictates the use of either some other cooling scheme for this region or another vane with a thicker trailing edge and larger trailing-edge wedge angle.

Concerning the latter alternative, another vane design for application in supersonic transport aircraft which has a thicker trailing-edge section is discussed in reference 14. Figure 10 shows an overlay of this vane scaled to the same axial chord length as the vane

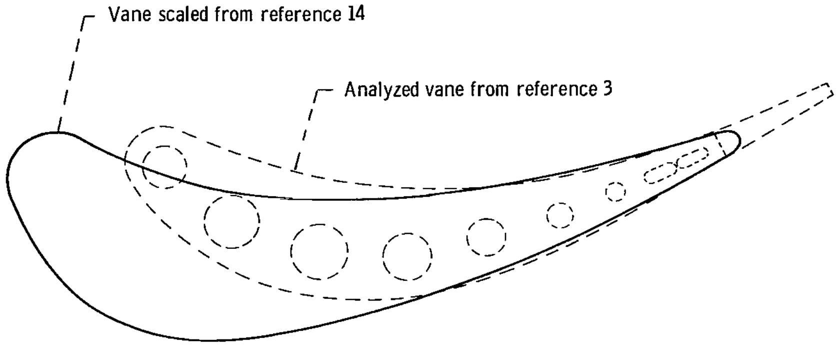


Figure 10. - Comparison of trailing-edge region of two vanes scaled to same axial chord length, turning angle, and free-stream inlet and exit Mach number.

analyzed. The turning angle and free-stream inlet and exit Mach number are the same for the two vanes. When the dimensions of the trailing edge of the alternative vane are compared to the minimum thickness successfully cooled on the analyzed vane, there is no size restriction to prohibit cooling the trailing-edge region with fuel.

A heat pipe was also considered for cooling the trailing-edge region. The application of heat pipes to turbine cooling using a liquid metal as a working fluid is discussed in references 15 to 17. The attractive feature of a heat pipe is that it can transfer large amounts of heat with very small temperature differences. The heat pipe operates at the boiling temperature of its working fluid. If a heat pipe with sodium as its operating fluid is placed in the trailing-edge region of the given vane, as illustrated in figure 11, the trailing-edge temperature would vary little from the $1622^{\circ}$ F (1157 K) sodium boiling point point at atmospheric pressure. The fuel could cool the condenser section of the heat pipe after passing through the nine cooling passages (resulting in the same temperature distribution as previously discussed except for the region near the truncated surface). In the case of methane, that portion of the heat pipe directly in contact with the fuel would require an insulation barrier to reduce its surface temperature below $1200^{\circ}$ F (922 K) to avoid carburization.

Heat pipe investigations for cooling turbine vanes are under consideration by various industrial concerns to determine methods of building heat pipes that will adequately cool under the heat fluxes that are encountered in high-temperature engine application. Further analysis of a heat pipe for methane- or hydrogen-cooled vanes was considered to be premature at this time.

Effects of perturbating the thermal design conditions. - The sensitivity of the local outside and inside surface temperatures (1) to changes in the thermal conductivity of the insulation, (2) to changes in the thickness of the insulation separating the outer vane shell and a cooling passage, and (3) to local loss of braze contact between the outer shell and insulation is an important factor in considering the fabrication and operation of the vane.

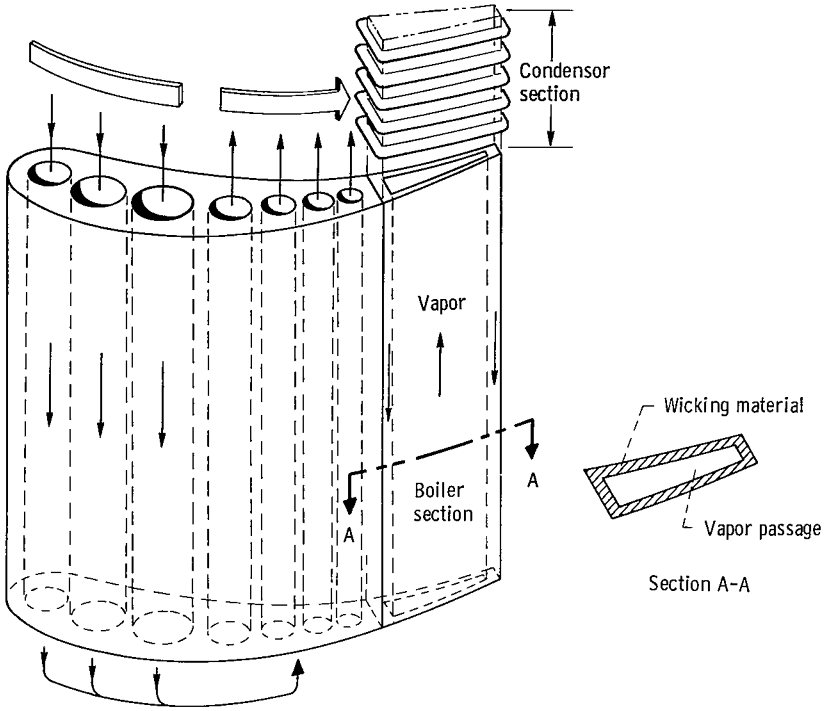


Figure 11. - Possible configuration of spanwise heat pipe for cooling trailing-edge region.

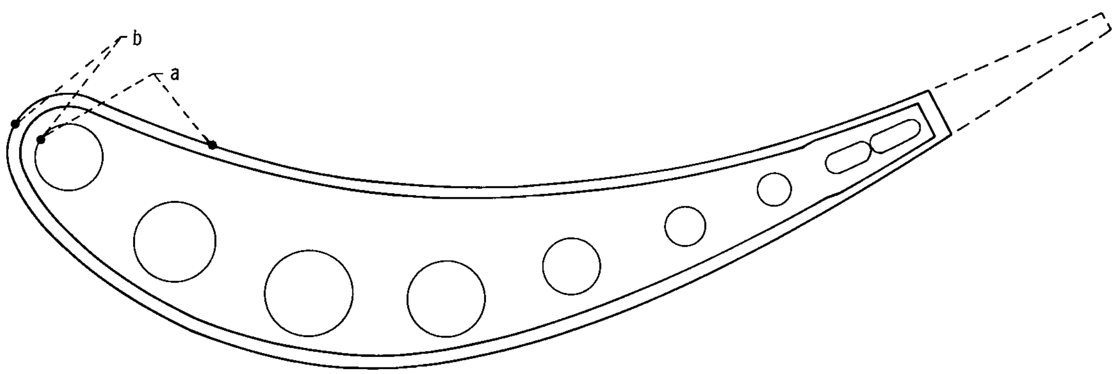


Figure 12. - Locations of maximum surface temperature sensitivity with respect to changes in (a) insulation thermal conductivity and (b) insulation thickness.

In this section the effect on the surface temperatures of independently changing these conditions is discussed for the case of methane-cooled vanes.

When the thermal conductivity of the insulation material was increased by 20 percent, the maximum temperature change on the inside and outside surfaces occurred at locations marked "a" in figure 12. At these locations, the outside surface temperature decreased by $78^{\circ}$ F (43 K) for takeoff conditions, while the inside surface temperature increased by $45^{\circ}$ F (25 K) for cruise conditions.

If a tolerance of ±0.003 inch (±0.076 mm) is maintained in the thickness of the insulation separating the leading-edge cooling passage from the outer shell, the following leading-edge surface temperature variation resulted (location designated "b" in fig. 12):

| Temperature variation, $^{\circ}$F (K) | | Location | Flight condition |
|---|---|---|---|
| $^{\circ}$F | K | | |
| ±11 | ±6 | Outside surface | Cruise |
| ±15 | ±8 | Outside surface | Takeoff |
| ∓13 | ∓7 | Inside surface | Cruise |
| ∓13 | ∓7 | Inside surface | Takeoff |

The largest increase in tł vane shell surface temperature caused by a local loss of contact between the shell and insulation occurs at the leading edge where the heat flux is maximum. Assuming an infinite contact resistance between the shell and insulation over the interface surface extending $10^{\circ}$ (0.175 rad) either side of the leading edge along the entire span length resulted in the following local increase in the leading-edge temperature: $68^{\circ}$ F (38 K) for cruise and $111^{\circ}$ F (62 K) for takeoff Even if the braze did fail, the contact resistance would not be infinite but these results represent the worst possible case.

The surface temperature sensitivities for the hydrogen-cooled vane were of the same order of magnitude as in the methane case.

## CONCLUDING REMARKS

Based on the analysis of the feasibility of cooling the first-stage stator of an SST aircraft directly with methane or hydrogen fuel, the following remarks can be made:

1. The analysis showed that it was possible from a thermal standpoint to use direct fuel cooling with hydrogen and methane in turbine stator vanes.

2. It was necessary to provide insulation between the fuel passages and the outer vane shell in order to control the shell temperatures and protect the fuel tubes from overheating. Excessive fuel surface temperatures may cause fuel cracking and carburization in the case of methane cooling.

3. It is difficult to cool a thin trailing edge directly with fuel because of the lack of sufficient thickness to accommodate the coolant passage and insulation. In some cases

the trailing-edge region may have to be shortened.

4. A fibrous metal appears to be a satisfactory insulation material. However, attaching it to the shell may be a problem. It has a range of thermal conductivity values, depending on its porosity, which are compatible with the values required for the insulation.

5. For the methane-cooled vane, the maximum external surface temperature and maximum external surface chordwise temperature variation at midspan were, respectively, $1802^{\circ}$ and $184^{\circ}$ F (1257 and 102 K) for cruise and $1938^{\circ}$ and $187^{\circ}$ F (1332 and 104 K) for takeoff. Similarly, the corresponding results for the hydrogen-cooled vane were respectively, $1659^{\circ}$ and $191^{\circ}$ F (1177 and 106 K) for cruise and $1902^{\circ}$ and $197^{\circ}$ F (1312 and 109 K) for takeoff.

6. The temperature difference across the vane shell (surrounding the insulation and cooling passages) at the leading edge was $48^{\circ}$ and $70^{\circ}$ F (27 and 39 K) for the methane-cooled vane at cruise and takeoff, respectively. The corresponding temperature differences for the hydrogen-cooled vane were $60^{\circ}$ and $74^{\circ}$ F (33 and 41 K).

7. The maximum fuel passage surface temperatures occurred for cruise conditions. At the vane midspan, these temperatures were $1070^{\circ}$ and $692^{\circ}$ F (850 and 640 K) for methane and hydrogen cooling, respectively.

8. The fuel temperature rise in passing all the fuel required by the combustor through the first-stage turbine stator was $340^{\circ}$, $135^{\circ}$, $165^{\circ}$, and $63^{\circ}$ F (189, 75, 92, and 35 K) for the respective cooling fuel - flight condition combinations of methane-cruise, methane-takeoff, hydrogen-cruise, and hydrogen-takeoff.

Lewis Research Center,
National Aeronautics and Space Administration,
Cleveland, Ohio, June 9, 1970,
720-03.

# APPENDIX A

## SYMBOLS

| | |
|---|---|
| $A$ | area |
| $C_p$ | specific heat |
| $D$ | coolant passage tube diameter |
| $\bar{h}_c$ | average vane-to-coolant heat transfer coefficient |
| $h_g$ | local gas-to-vane heat transfer coefficient |
| $h_{ms}$ | midspan fuel enthalpy |
| $h_o$ | fuel enthalpy entering a cooling passage |
| $k$ | thermal conductivity |
| $n$ | node number |
| Pr | Prandtl number, $\mu C_p/k$ |
| $q_i$ | rate of heat transferred to coolant flowing in $i^{th}$ passage between root or tip and midspan |
| Re | Reynolds number, $\rho VD/\mu$ |
| $T$ | temperature |
| $\bar{T}_{c,e}$ | average compressor exit temperature |
| $\bar{T}_t$ | average turbine inlet temperature |
| $T_{t,max}$ | turbine inlet hot-spot temperature |
| $V$ | velocity |
| $w$ | flow rate |
| $\mu$ | viscosity |

Subscripts:

| | |
|---|---|
| b | property evaluated at bulk temperature |
| c | coolant |
| i | cooling passage number |
| ms | midspan |
| o | upstream end of cooling passage |
| s | property evaluated at surface temperature |

# APPENDIX B

## NUMERICAL METHOD

The steady-state two-dimensional heat conduction equation with constant thermal conductivity,

$$\frac{\partial^2 T}{\partial x^2} + \frac{\partial^2 T}{\partial y^2} = 0 \tag{B1}$$

is solved numerically by an iterative over-relaxation method. The vane is broken into a grid of N nodes or material lumps (either rectangular or irregular in shape).

Consider an energy balance on a typical $n^{th}$ node ($n = 1, 2, \ldots, N$) shown rectangular in the following sketch for simplicity:

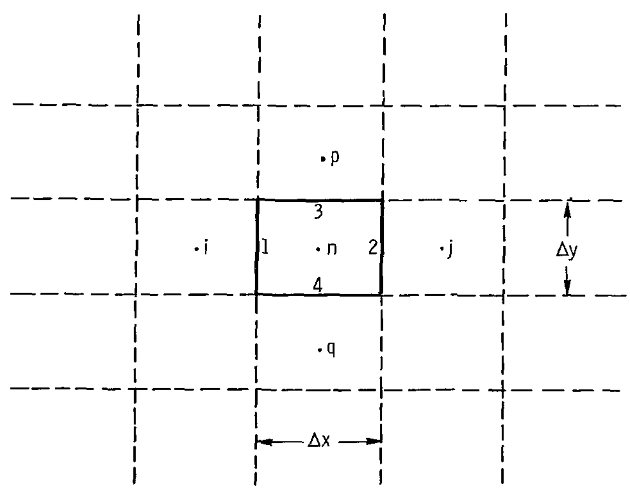


(Unit depth in the z-direction)

For no internal heat generation,

$$\sum_{S=1}^{4} A_{n,s} U_{n,s} (T_e - T_n) = 0 \tag{B2}$$

where

S face number

$A_{n,s}$ area of S face of node n

$l$ number of node adjacent to side S of node n

$U_{n,s}$ thermal conductance between node n and node adjacent to side S

Consistent with the sketch,

$$
\left.
\begin{aligned}
A_{n,1} &= A_{n,2} = \Delta x\, \Delta y \\
A_{n,3} &= A_{n,4} = \Delta y \cdot 1 \\
U_{n,1} &= U_{n,2} = \frac{k}{\Delta x} \\
U_{n,3} &= U_{n,4} = \frac{k}{\Delta y}
\end{aligned}
\right\} \qquad \text{(B3)}
$$

(For a boundary node with convection, U would be the local heat transfer coefficient and $T_l$ would be the fluid temperature.) Substituting equations (B3) into equation (B1) gives

$$k\left[\frac{\Delta y \cdot 1}{\Delta x}(T_i - T_n) + \frac{\Delta y \cdot 1}{\Delta x}(T_j - T_n) + \frac{\Delta x \cdot 1}{\Delta y}(T_p - T_n) + \frac{\Delta x \cdot 1}{\Delta y}(T_q - T_n)\right] = 0$$

Dividing by the elemental volume, $\Delta V = \Delta x\, \Delta y \cdot 1$ gives

$$\left[\frac{T_i - 2T_n + T_j}{(\Delta x)^2}\right] + \left[\frac{T_p - 2T_n + T_q}{(\Delta y)^2}\right] = 0 \qquad \text{(B4)}$$

Noting that

$$\lim_{\Delta x \to 0} \frac{T_i - 2T_n + T_j}{(\Delta x)^2} = \left.\frac{\partial^2 T}{\partial x^2}\right|_n$$

and similarly with y, in the limit as the node size becomes infinitesimally small, the difference equation tends to the differential equation (1). Let

$$E_n = \sum_s U_{n,s} A_{n,s} (T_l - T_n)$$

and

$$E_T = \sum_{n=1}^{N} |E_n|$$

As the solution converges, $E_T$ tends to zero.

If $T'_n$ is the new node temperature while $T_n$ is the temperature of node n from the previous iteration, then

$$\Delta T_n = T'_n - T_n$$

is the change in the temperature of node n between iterations. An overrelaxation factor $\gamma$, is introduced in the following equation to enhance convergence:

$$T'_n = T_n + \gamma \, \Delta T_n \tag{B5}$$

The iteration procedure using equations (B2) and (B5) is continued until $E_T$ becomes arbitrarily small.

## REFERENCES


1. Stepka, Francis S.: Considerations of Turbine Cooling Systems for Mach 3 Flight. NASA TN D-4491, 1968.
2. Whitlow, John B., Jr.; Eisenberg, Joseph D.; and Shovlin, Michael D.: Potential of Liquid-Methane Fuel for Mach-3 Commercial Supersonic Transports. NASA TN D-3471, 1966.
3. Burggraf, F.; Murtaugh, J. P.; and Wilton, M. E.: Design and Analysis of Cooled Turbine Blades. Part 2: Convection Cooled Nozzles and Buckets. Rep. R68AEG102, General Electric Co. (NASA CR-54514), Jan. 1, 1968.
4. Maxwell, J. B.: Data Book on Hydrocarbons. D. Van Nostrand Co., Inc., 1950.
5. Anon.: Thermodynamic Properties of Methane-Nitrogen Mixtures. Res. Bull. No. 21, Institute of Gas Technology, Feb. 1955.
6. Sieder, E. N.; and Tate, G. E.: Heat Transfer and Pressure Drop of Liquids in Tubes. Ind. Eng. Chem., vol. 28, no. 12, Dec. 1936, pp. 1429-1435.
7. Anon.: Investigations of Light Hydrocarbon Fuels with Flox Mixtures as Liquid Rocket Propellants. Rep. PWA-FR-1207, Pratt & Whitney Aircraft, 1965.
8. Woolley, Harold W.; Scott, Russell B.; and Brickwedde, F. G.: Compilation of Thermal Properties of Hydrogen in its Various Isotopic and Ortho-Para Modifications. J. Res. Nat. Bur. Standards, vol. 41, no. 5, Nov. 1948, pp. 379-475.
9. Hilsenrath, Joseph; et al.: Tables of Thermal Properties of Gases. Circular 564, National Bureau of Standards, Nov. 1, 1955.
10. Hendricks, Robert C.; Graham, Robert W.; Hsu, Yih Y.; and Friedman, Robert: Experimental Heat-Transfer Results for Cryogenic Hydrogen Flowing in Tubes at Subcritical and Supercritical Pressures to 800 Pounds per Square Inch Absolute. NASA TN D-3095, 1966.
11. Varga, Richard S.: Matrix Iterative Analysis. Prentice-Hall, Inc., 1962.
12. Anon.: Hydrocarbon SCRAMJET Feasibility Program. Vol. 1. Engine and Cooling Investigations. Rep. 6129, Marquardt Corp. (AFAPL-TR-67-97, vol. 1, DDC No. AD-384567L), Sept. 1967.
13. Danforth, C. E.; and Burggraf, F.: Design and Analysis of Cooled Turbine Blades. Part 5: Life Prediction of Selected Designs. Rep. R68AEG105, General Electric Co. (NASA CR-72417), Aug. 1968.

14. Whitney, Warren J.; Szanca, Edward M.; Moffitt, Thomas P.; and Monroe, Daniel E.: Cold-Air Investigation of a Turbine for High-Temperature-Engine Application. NASA TN D-3751, 1967.

15. Silverstein, Calvin C.: Preliminary Evaluation of Gas Turbine Regenerators Employing Heat Pipes. Silverstein Consultant (USAAVLABS-TR-68-10, DDC No. AD-671028), Apr. 1968.

16. Ogale, Vilas Avadhut: On the Application of the Semi-Closed Thermosyphon System to Gas Turbine Blade Cooling. Ph.D. Thesis, Technische Hogeschool, Delft, 1968.

17. Moussez, Claude; and Mihail, Arlette: Le Caloduc et le Thermosiphon Pour le Refroidissement des Aubes de Turbines à Gaz. Entropie, Sept.-Oct. 1966, pp. 102-109.



NASA-Langley, 1970 — 33 E-5701

NATIONAL AERONAUTICS AND SPACE ADMINISTRATION
WASHINGTON, D. C. 20546

OFFICIAL BUSINESS

**FIRST CLASS MAIL**

POSTAGE AND FEES PAID
NATIONAL AERONAUTICS AND
SPACE ADMINISTRATION

030 001 58 51 3DS 70272 00903
AIR FORCE WEAPONS LABORATORY /WLOL/
KIRTLAND AFB, NEW MEXICO 87117

ATT E. LOU BOWMAN, CHIEF,TECH. LIBRARY

POSTMASTER: If Undeliverable (Section 158 Postal Manual) Do Not Return

*"The aeronautical and space activities of the United States shall be conducted so as to contribute . . . to the expansion of human knowledge of phenomena in the atmosphere and space. The Administration shall provide for the widest practicable and appropriate dissemination of information concerning its activities and the results thereof."*

—NATIONAL AERONAUTICS AND SPACE ACT OF 1958

# NASA SCIENTIFIC AND TECHNICAL PUBLICATIONS

TECHNICAL REPORTS: Scientific and technical information considered important, complete, and a lasting contribution to existing knowledge.

TECHNICAL NOTES: Information less broad in scope but nevertheless of importance as a contribution to existing knowledge.

TECHNICAL MEMORANDUMS: Information receiving limited distribution because of preliminary data, security classification, or other reasons.

CONTRACTOR REPORTS: Scientific and technical information generated under a NASA contract or grant and considered an important contribution to existing knowledge.

TECHNICAL TRANSLATIONS: Information published in a foreign language considered to merit NASA distribution in English.

SPECIAL PUBLICATIONS: Information derived from or of value to NASA activities. Publications include conference proceedings, monographs, data compilations, handbooks, sourcebooks, and special bibliographies.

TECHNOLOGY UTILIZATION PUBLICATIONS: Information on technology used by NASA that may be of particular interest in commercial and other non-aerospace applications. Publications include Tech Briefs, Technology Utilization Reports and Notes, and Technology Surveys.

*Details on the availability of these publications may be obtained from:*

**SCIENTIFIC AND TECHNICAL INFORMATION DIVISION**

**NATIONAL AERONAUTICS AND SPACE ADMINISTRATION**

**Washington, D.C. 20546**